NORTH-HOLLAND

An Application of Fuzzy Logic Control to a Gimballed Payload on a Space Platform

STANLEY E. WOODARD

NASA Langley Research Center, Hampton, VA 23681

DEVENDRA P. GARG

Department of Mechanical Engineering and Materials Science, Duke University, Durham, NC 27706

and

CHING YU TYAN and PAUL P. WANG

Department of Electrical Engineering, Duke University, Durham, NC 27706

ABSTRACT

This paper will present results of applying two autonomous fuzzy controllers to a dynamically coupled system. The system consists of a space platform and a gimballed payload. The controllers are developed with the systems decoupled. Parametric studies are performed on the support limits for the error, change-in-error, and control. These parametric variations provide insight into satisfactorily tuning the controllers. The controllers were compared to controllers developed using Linear Quadratic Regulator (LQR) control design. The controllers are used to perform slew maneuvers and disturbance rejection. A design procedure using constraints due to hardware or software specification is also examined. When error and control support limits are specified, tuning the fuzzy controller is made relatively easy. The systems were coupled and the response of the payload and platform were examined for commanded payload trajectories and impulses applied to the platform. The fuzzy controllers performed very well in all cases.

INTRODUCTION

The advent of multipayload spacecraft with elastically flexible appendages has made it critical that spacecraft designers have a knowledge

INFORMATION SCIENCES 4, 143–165 (1995)

655 Avenue of the Americas, New York, NY 10010

0020-0255/95/$9.50
SSDI 0020-0255(95)00165-L

of the mutual interactions of the payloads as well as any control-structures interaction [1–5]. The ultimate design objective is to meet the pointing requirements at the boresight of each science instrument. The goal of this study is to use fuzzy logic control as a means to maintain either a constant slew rate or fixed line-of-sight pointing for a gimballed payload mounted on a space platform subject to vibration due to multiple disturbance sources. Autonomous fuzzy logic controllers will be used to maintain a desired line-of-sight pointing for a gimballed payload and to maintain a desired attitude for the spacecraft. To achieve this objective, one must understand how each instrument and subsystem contributes to the overall spacecraft dynamic response. This knowledge will be beneficial to the design of future multipayload spacecraft.

To date, almost all fuzzy logic controllers (FLC) use only "if–then" rules. The overall scheme of using FLC for feedback error control is to generate a control input based upon error information resulting from feedback [6–9]. The control input to the system is a desired or referenced input. Conceptually, FLC is similar to traditional feedback control, except that the fuzzy controller requires the user to formulate membership functions for various fuzzy sets, develop rules that map input conditions to responses using fuzzy sets, and select fuzzification and defuzzification techniques for a small number of options. The advantage of using fuzzy controllers is that they have been shown to produce very good results in cases where the mathematical description may not be readily available or the description may be of questionable fidelity [10–14]. Fuzzy logic controllers also allow a designer to take advantage of the concept of constraints in system specification. The system used in this study has several constraints that reflect the physical implementation of this system such as the payload's gimbal motor bandwidth and torque level, maximum excursion of payload allowed by the gimbal, and spacecraft attitude control system bandwidth.

This study will present the results of using FLC on a space platform with a gimballed payload. To date, individual fuzzy controllers have been used on autonomous systems. This paper will present results of applying two autonomous fuzzy controllers to a dynamically coupled system. Traditionally, spacecraft design is done with each subsystem and its respective controller developed autonomously. Afterward, the subsystems are integrated. In this paper, results will be presented that show the combined dynamics of two subsystems which are dynamically coupled, but autonomously controlled. The systems are coupled via a gimballed drive shaft, a variable mass matrix (which can be ignored for small payload gimballed inertia/spacecraft inertia ratios), and coupling of the spacecraft attitude motion to the payload elevation.

FUZZY LOGIC CONTROL DEVELOPMENT

Fuzzy logic control extends fuzzy set theory to the control of processes [6–9]. The basic architecture for fuzzy logic control is depicted in Figure 1. As shown in Figure 1, outputs from the controlled system are input to a fuzzification process. This fuzzification process maps the input to memberships of fuzzy sets. Fuzzification relates vague and imprecise inputs to approximate reasoning. Fuzzy controllers developed to date employ a variety of inputs. In this study, error and change-in-error about a trajectory of set points will be used to describe the development of a fuzzy controller. Fuzzy membership functions are shown in Figure 2. These memberships are used for the error, change-in-error, and control output. The fuzzy term sets are positive big (PB), positive small (PS), zero (Z), negative small (NS), and negative big (NB). These sets are symmetric about zero and are bounded by minimum and maximum support limits. For example, if the fuzzy sets are for error, the support is all quantities which can be measured between the limits (minimum support and maximum support values) of the measurement apparatus. For any element, x_0, in the support of the fuzzy sets, its grade of membership to the fuzzy sets is $\mu(x_0)$. The membership functions have an overlap at grade 0.5. This overlap gives all support elements membership in two term sets unless the support element has membership grade of 1.0 in any term set. Because of the overlap, the

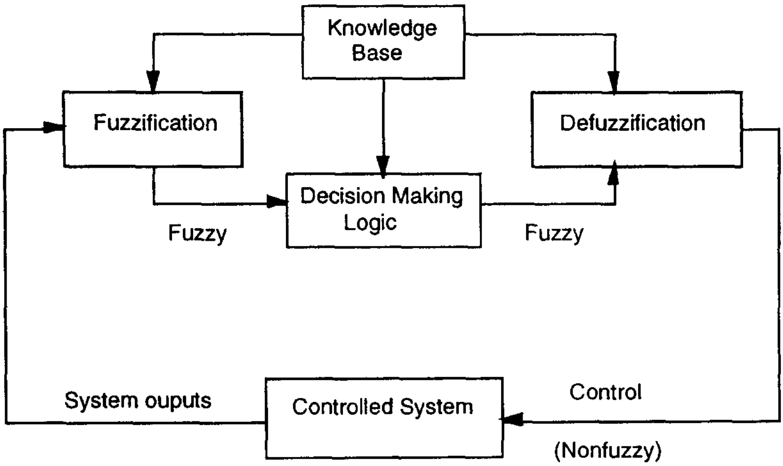

Fig. 1. Fuzzy logic control.

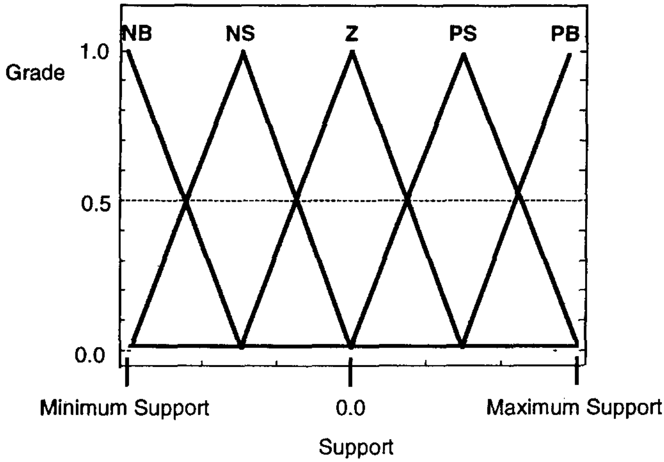

Fig. 2. Fuzzy membership functions on symmetric universe of discourse.

control gradient with respect to the error and change-in-error is continuous, monotonic, and never zero [15]. The advantage this fuzzy membership offers is the effect that the membership functions have when the support elements are near zero. Unless the element is absolutely zero, the elements have nonzero grades on the respective side of zero. The result is a smooth approach to zero for process output as the support elements approach zero.

Prior knowledge of the process can be used to design the membership function (granularity and linguistic variables). This knowledge base could be a process model, self organization, operator's knowledge, and expert knowledge/experience. For example, the granularity should reflect how fast the inputs are changing. Following the fuzzification process is decision making logic where control action is predicated from rules of inference. The decisions are predicated on the input. As an example, if "input is A," then "output should be B." Control rules are given in Figure 3. These rules are written in matrix form and interpreted as

If error is PS and change-in-error is Z, then control output is NS.

The output of inference is fuzzy and defuzzified in a defuzzification process,

$$u = \frac{\sum_{i=1}^{q} x_i \, \mu_B(x_i)}{\sum_{i=1}^{q} \mu_B(x_i)}$$

ERROR \ CHANGE-IN-ERROR	PB	PS	Z	NS	NB
PB	Z	NS	NB	NB	NB
PS	PS	Z	NS	NB	NB
Z	PB	PS	Z	NS	NB
NS	PB	PB	PS	Z	NS
NB	PB	PB	PB	PS	Z

Fig. 3. Control rule matrix used for space platform and payload controllers.

with q as the quantization level of the output, x_i is the output at the quantization level q, the ith membership grade is $\mu_B(x_i)$, and u is the crisp output value given to the control actuator.

The controllers for the payload and the platform are structurally similar. Control is predicated upon a measured error and change in error. The membership functions depicted in Figure 2 are used for the payloads and platform's error, change-in-error, and control. The design objective is to develop the appropriate minimum and maximum support limits for each membership function. Since the membership functions are symmetric, the minimum and maximum support limits are equal in magnitude and opposite in sign. Each controller has a set of three support limits for error,

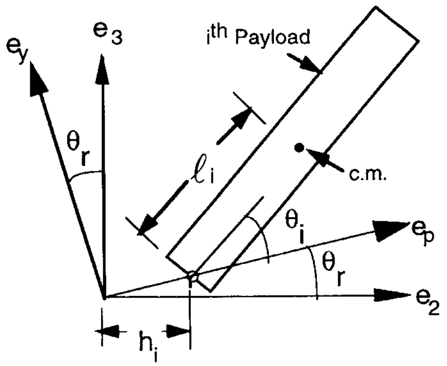

Fig. 4. Platform and Payload Coordinate System.

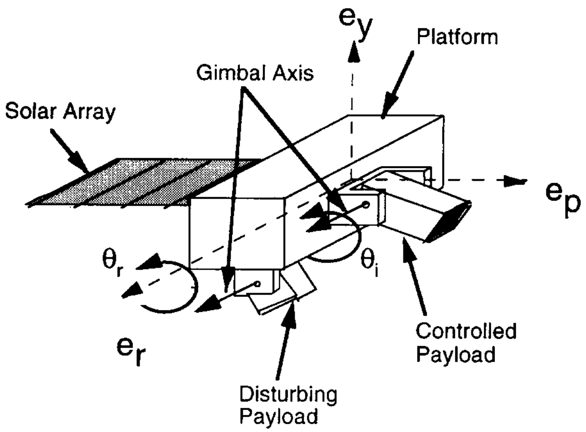

Fig. 5. Space platform with gimballed payloads.

change-in-error, and control output. These are E, ΔE, and C, respectively. The objective of the controller design is to develop the appropriate set of support limits to give the desired performance. The control rule matrix given in Figure 3 will be used for both the payload and platform controllers.

SYSTEM MODEL

A dynamic model of a spacecraft with multiple gimballed payloads and a flexible appendage has been developed. The system is depicted in Figures 4 and 5. The system consists of two single-axis (elevation) gimballed payloads mounted on a rigid platform. One payload is an open-loop subsystem. Its motion imparts a disturbance about the roll axis. The other payload is a closed-loop subsystem whose elevation, θ_i, relative to the platform follows a commanded trajectory. Each payload has a mass and inertia, m_i and I_i, respectively. The gimbal mounts are offset, h_i, from the platform roll axis, e_r. Each payload's center of mass is offset, l_i, from the gimbal mount. All disturbances are assumed about the spacecraft's roll axis (e_r on Figure 5). A Lagrangian formulation yields the following equations describing the platform's roll motion, θ_r, and the motion of the ith payload, θ_i, when generalized torques, Q_{θ_r} and Q_{θ_i} are applied to the platform and payload. The generalized torques can be modeled as ramps, steps, impulses, sinusoidal forces or periodic force inputs, or combinations of the above.

$$I_r\ddot{\theta}_r + \sum_{i=1}^{n} I_i\left(\ddot{\theta}_r + \ddot{\theta}_i\right) + \sum_{i=1}^{n} m_i\Big[l_i^2\ddot{\theta}_r + h_i^2\ddot{\theta}_r$$

$$+ l_i^2\ddot{\theta}_i + l_i h_i \ddot{\theta}_i \cos\theta_i + 2l_i h_i \ddot{\theta}_r \cos\theta_i - 2l_i h_i \dot{\theta}_r \dot{\theta}_i \sin\theta_i - l_i h_i \theta_i^2 \sin\theta_i\Big]$$

$$+ k\theta_r = Q_{\theta_r} \tag{1}$$

$$I_i\left(\ddot{\theta}_r + \ddot{\theta}_i\right) + m_i\left[l_i^2\ddot{\theta}_r + l_i^2\ddot{\theta}_i + l_i h_i \ddot{\theta}_r \cos\theta_i + l_i h_i \dot{\theta}_r^2 \sin\theta_i\right] = Q_{\theta_i}. \tag{2}$$

The platform has an inertia, I_r, and torsional stiffness, k, about the roll axis. The system of equations is linearized about a configuration of all generalized coordinates being zero. The payload and platform inertia are 3.5 and 11,890 lb-ft^2, respectively. The ith payload motion equation is given to show the dynamic coupling of the payload and the platform. Transfer functions are developed between each payload disturbance and the platform to ascertain how each contributes to the overall vibration, and thus jitter of the platform. Jitter is the measure of how much the spacecraft attitude has changed in a reference time interval. Because this study is only concerned with spacecraft jitter, environmental disturbances such as solar pressure, aerodynamic drag and torques, gravity-gradient torques, and the dynamic effect due to the Earth's oblateness are considered to be negligible.

The dynamic coupling between the closed-loop payload and the platform is summarized in Figure 6. In the absence of any torsional mode (mostly due to environmental influences such as gravity-gradient torques), the disturbance torques imparted to either payload drive shaft is only imparted to the spacecraft and the respective payload, but not to the opposite payload. Therefore, any drive shaft torque will cause a change in spacecraft roll attitude and rate. Since both gimbals are attached to the platform, the change in spacecraft roll attitude and rate will cause the opposite payload's line-of-sight to move correspondingly. Thus, although there is no direct transfer of torque from one payload to the other, there is a change in line-of-sight pointing of one payload due to the disturbance of the other. Torques applied about the spacecraft roll axis are not directly transferred to the payload gimbal shafts, but result in a change of spacecraft roll attitude and rate. The torques perturb the payloads line-of-sight pointing correspondingly. When a torque is applied to any drive shaft, the

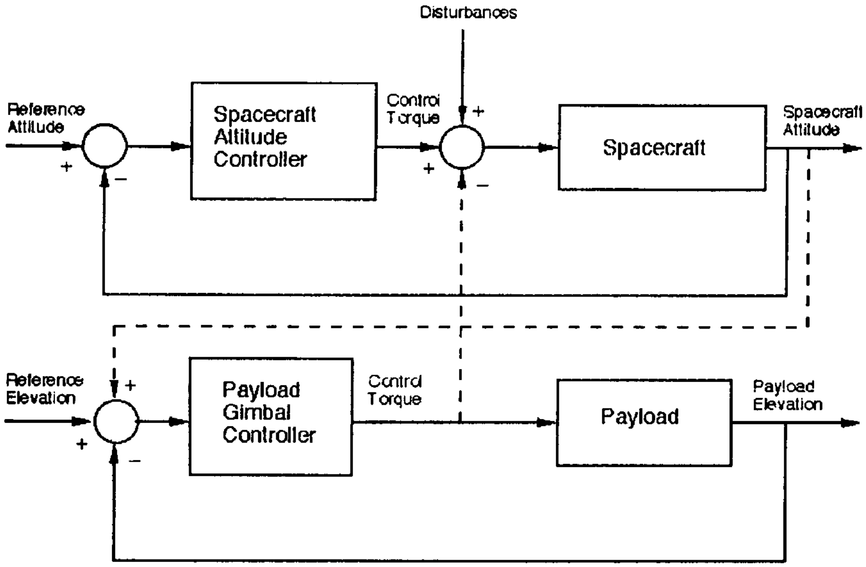

Fig. 6. Payload and platform dynamic coupling.

subsequent changes in position and rate of the platform and the payload are proportional to the inertia of the platform and the payload, respectively, resolved to the gimbal position. Thus, the payload–platform inertia ratio (using inertia resolved to the gimbal) is also the ratio between payload rotation angle and the change in spacecraft attitude.

In modeling the system, flexible appendages with multiple modes were not considered as part of the platform, but as a contributor to spacecraft jitter. This is because once they are excited, the subsequent bending moments imparted to the spacecraft at the root of the appendage have the same effect as any other disturbance applied to the platform. By the very basic definition of jitter given earlier, it does not matter how an instrument's boresight line-of-sight varies during a given time: it only matters that it varies. For nongimballed instruments, any motion to the platform is a jitter source.

PLATFORM CONTROLLER DESIGN

Spacecraft attitude controllers typically maintain or adjust a spacecraft's attitude with respect to the Earth's zenith and the spacecraft's velocity vector. When the platform is modeled separately from the payloads, the equation of motion reduces to

$$I_r \ddot{\theta}_r = Q_{\theta_r}$$

or

$$\ddot{\theta}_r = I_r^{-1} Q_{\theta_r}. \tag{3}$$

The equation can be placed in first-order form as

$$\dot{x} = Ax + Bu \tag{4}$$

with

$$x = \begin{bmatrix} \theta_r & \dot{\theta}_r \end{bmatrix}, \tag{5}$$

$$A = \begin{bmatrix} 0 & 1 \\ 0 & 0 \end{bmatrix}, \tag{6}$$

$$B = \begin{bmatrix} 0 \\ I_r^{-1} \end{bmatrix}, \tag{7}$$

and

$$u = Q_{\theta_r}. \tag{8}$$

The control torque, u, is the output from the defuzzification step of the fuzzy logic controller. As a means of comparison, the results of the fuzzy logic controller are compared to the result of using a controller developed using Linear Quadratic Regulator.

Linear Quadratic Regulator control is developed using optimal control theory. The optimal control, u, which minimizes the performance index

$$J = \int_0^{\infty} (x^T Q x + u^T R u)\, dt \tag{9}$$

is given by

$$u = -(R^{-1} B^T P) x = -Kx \tag{10}$$

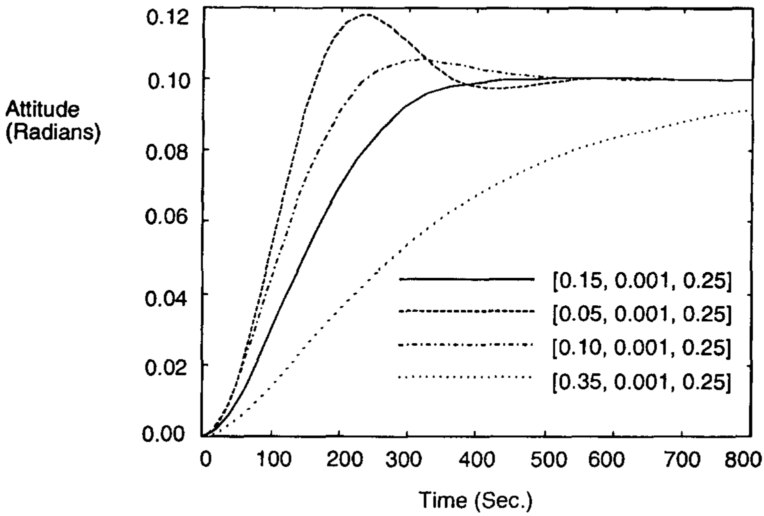

Fig. 7. Platform attitude response due to error support variations.

where Q is the positive-semi-definite state penalty matrix, R is the positive-definite control penalty matrix, and P is the positive-definite solution to the steady-state Riccati matrix equation,

$$-PA - A^T P + PBR^{-1}B^T P - Q = 0. \tag{11}$$

Using an identity matrix for the weight, Q, and unity for the weight, R, the position and weight gains are [1 154.21], respectively.

The platform controller is designed for two modes of operation: slew maneuvers (changing attitude) and attitude control. As mentioned earlier, the approach used to design the fuzzy controllers is to use the membership functions given in Figure 2 and the control rules given in Figure 3. The design variables are the support limits for error, E, change-in-error, ΔE, and control, C. Each variable was varied while the other two remained constant to ascertain the effect it had on the attitude response. Results of varying the error support limits are shown in Figure 7. The platform is commanded to slew 0.1 radians and maintain 0.1 radians as its new attitude. The support limit set [0.15, 0.001, 0.25] resulted in a response which approached 0.1 radians in approximately 440 sec. The other cases either had overshoot or did not approach the commanded position until after 800 sec. The observed trend was that as the error limit became smaller, the overshoot decreased and the damping increased. Change-in-

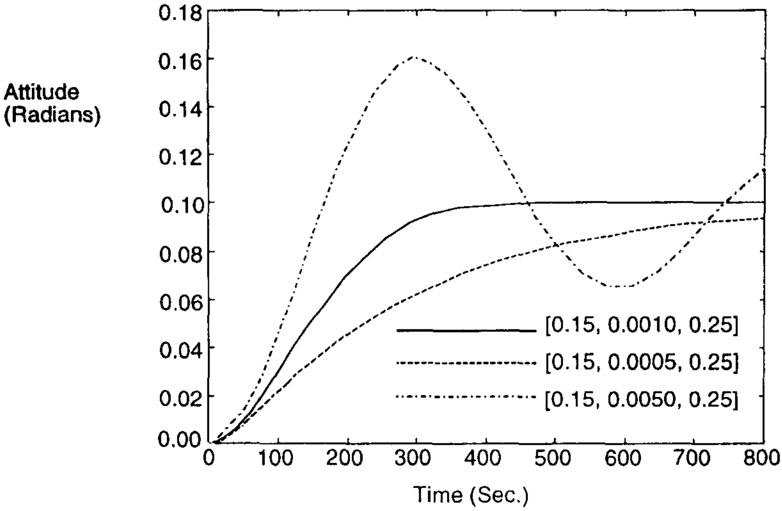

Fig. 8. Platform attitude response due to change-in-error support variations.

error variations are shown in Figure 8. Similar to changing the error support, decreasing the change-in-error limit increased the damping of the response. Figure 9 shows the result of varying the control support limit. Although the response did not vary significantly, the response trend indicates that larger support limits result in a longer transition to the commanded position.

The fuzzy platform controller is compared to that using LQR in Figures 10, 11, and 12. In Figure 10, the platform is commanded to reposition and maintain 0.5 radians. The fuzzy support limits are [0.15, 0.001, 0.25]. Although the LQR approached the commanded position much faster, the fuzzy controller approached the commanded position without any overshoot. However, the fuzzy controller begins to maintain the commanded position much sooner than the LQR. In Figure 11, the fuzzy controller repositioned the platform 0.1 radians more quickly than the LQR and without any overshoot. Attitude control in the presence of a disturbance is shown in Figure 12. The platform is given an unit impulse and commanded to maintain a position of 0.0 radians. The fuzzy controller results in less excursion from the commanded position and a quicker settling time. In Figure 12 is shown the sensitivity of the fuzzy and LQR controllers to spacecraft inertia. The fuzzy controller was less sensitive to variation in inertia. Each controller was examined using the nominal inertia of 11, 890

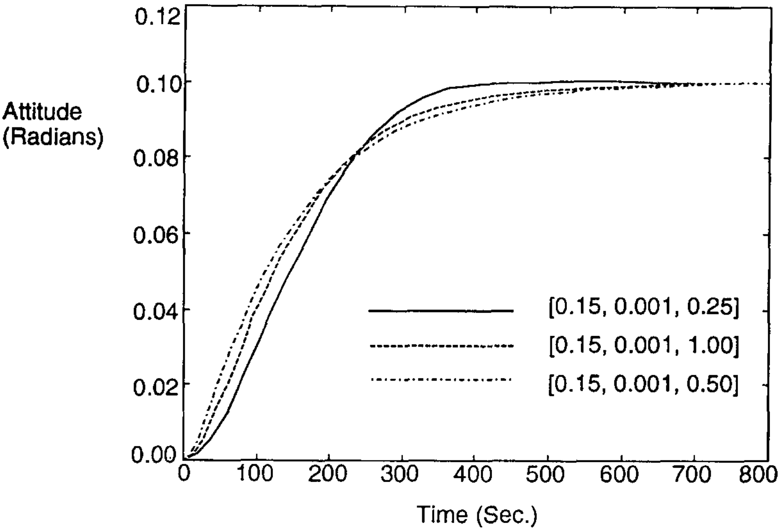

Fig. 9. Platform attitude response due to control support variations.

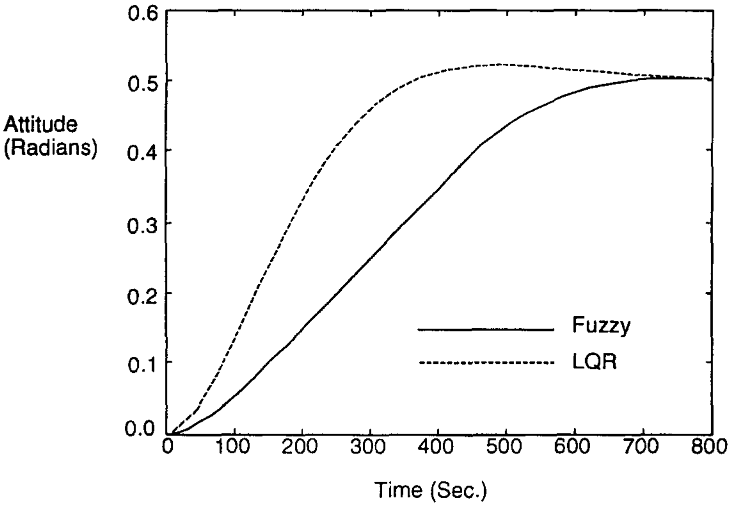

Fig. 10. Platform attitude for a commanded gimbal angle of 0.5 radians using fuzzy control and LQR control.

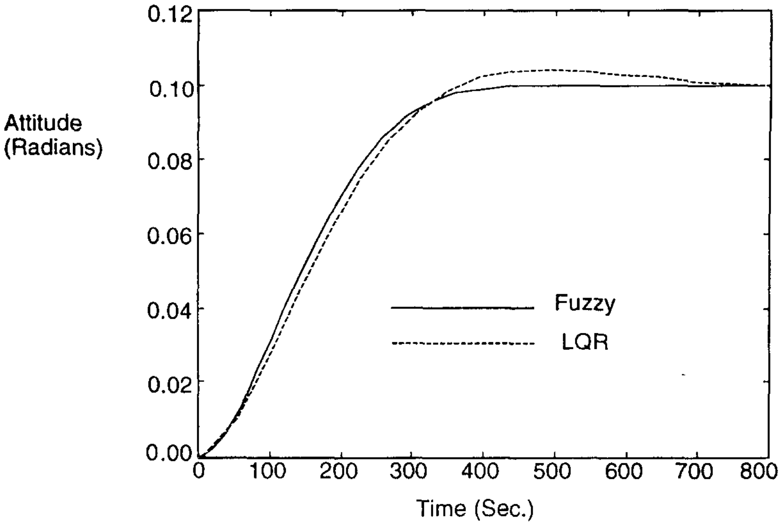

Fig. 11. Platform attitude for a commanded gimbal angle of 0.1 radians using fuzzy control and LQR control.

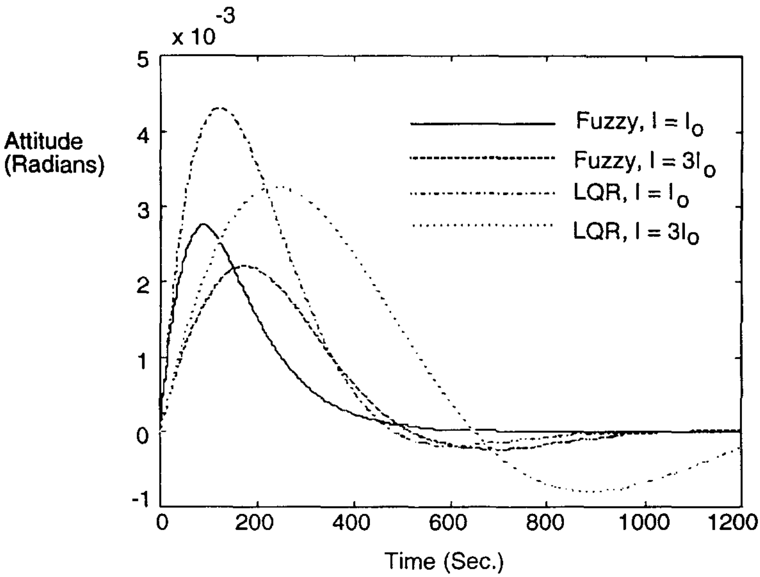

Fig. 12. Platform response to unit impulse.

lb-ft^2 and an inertia which was three times the nominal inertia. The fuzzy control resulted in a response amplitude which was less than the response using the LQR for both cases of inertia. Response settling time of the fuzzy controller for the case of triple the inertia was comparable to the LQR controller using the nominal inertia.

CONTROLLER DESIGN USING PHYSICAL SPECIFICATIONS

An important consideration in the design of control systems is that of constraints. These could be physical limitations in hardware or software such as controller torque output (magnitude vs. frequency), measurement sampling rate, measurement sampling range (i.e., limits), etc. Fuzzy membership support limits are naturally malleable to some system specifications such as error and control output. The control support limit can be set using the physical limitations of the process hardware. Error support limits could be sized be the measurement range.

If prior knowledge of the controller's output limitation and measurement range is available, a fuzzy logic controller can be tuned by having the control support limits as the controller's output limitation. The error support limitation could be either the physical measurement limit or it could reflect bounds of measurement within a given regime of operation. After the error and control support limits are set, tune the change-in-error support limit until it results in the desired response. In Figure 13, the

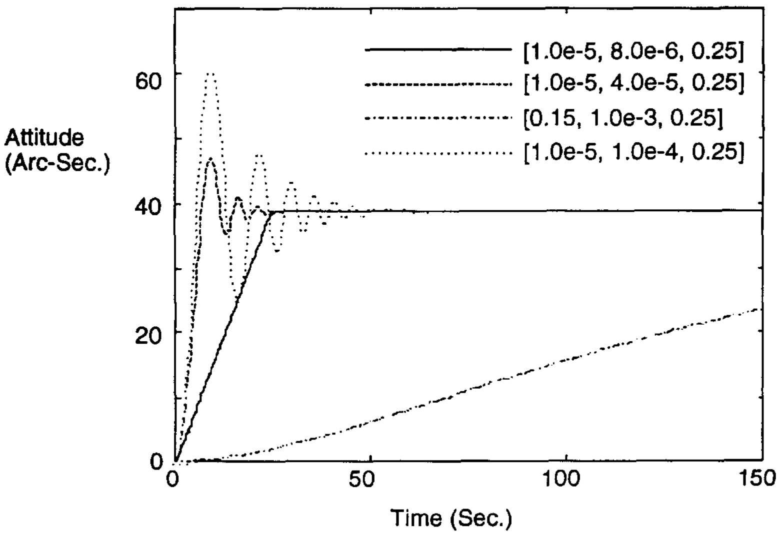

Fig. 13. Platform attitude response to commanded position of 40 arc-sec.

results of using such an approach are shown. The platform is commanded to transition to and maintain 40 arc-sec (1.939E-4 radians). Such a range of motion is typical for maintaining an attitude, but not for slew maneuvers [which are long duration (0.067 degrees per second)]. The fuzzy support which gives the desired performance for maneuvers greater than 0.1 radians has very poor performance for a 40 arc-sec maneuver. However, if the range of measurement is set to -1.0E-5 to 1.0E-5, the control rules are more sensitive. Furthermore, once the error range and control range are set, the change-in-error support limit can be tuned as in Figure 13.

PAYLOAD CONTROLLER DESIGN

The design development of the payload controller is similar to that of the platform. When developed separately, the payload equation of motion is

$$(I_i + m_i l_i^2)\ddot{\theta}_i = Q_{\theta_i}.$$

Using Linear Quadratic Regulator design and the same weights used for the platform, the position and rate gains for the platform roll controller are [1 2.8284].

The payload controller is designed for two modes of operations: slew maneuvers and disturbance rejection. Disturbance rejection for the payload is for both impulses and periodic disturbances. Similar to the platform, parameter variations were performed on the payload controller's error, change-in-error, and control support limits. The variations are shown in Figure 14–16, respectively. The same trends were observed with the payload response that were observed with the platform response. To examine disturbance rejection, a periodic disturbance of 0.01 ft-lb at 0.25 Hz was placed about the payload's elevation drive shaft. In Figure 17, it can be seen that the fuzzy controller performed much better at compensating for the disturbance. The peak excursions from the commanded position of 0.5 radians using fuzzy logic were half those when LQR was used to control the payload elevation. In Figures 18 and 19 are responses of using fuzzy and LQR controllers for a slew maneuver and compensating for a unit impulse, respectively. Similar to the platform, the fuzzy controller produced much better results.

Payload elevation control was also developed using design specifications on the error and control support limits. Here, it is assumed that the maximum torque available is 0.03 ft-lb, and that the maximum error measurement is 0.15 radians (8.59 degrees). Thus, it is only necessary to tune the change-in-error limit. This is shown in Figure 20. Furthermore, once the system is tuned, the error limits can be readjusted as in Figure 21.

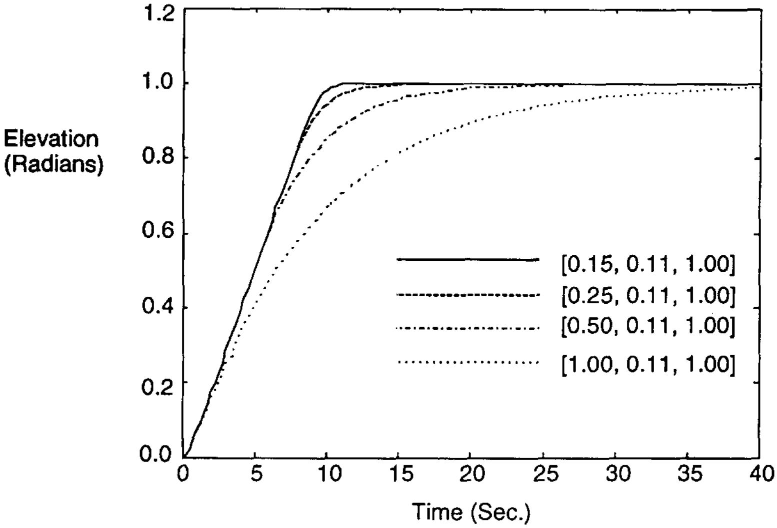

Fig. 14. Payload elevation response due to error support variations.

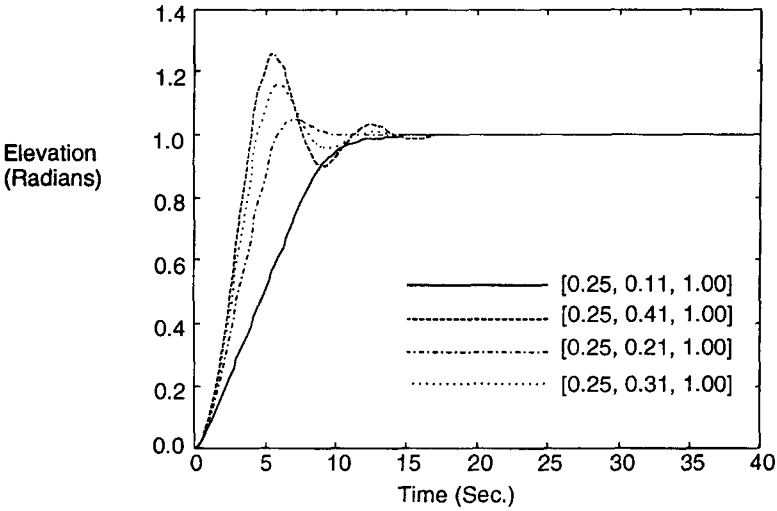

Fig. 15. Payload elevation response due to change-in-error support variations.

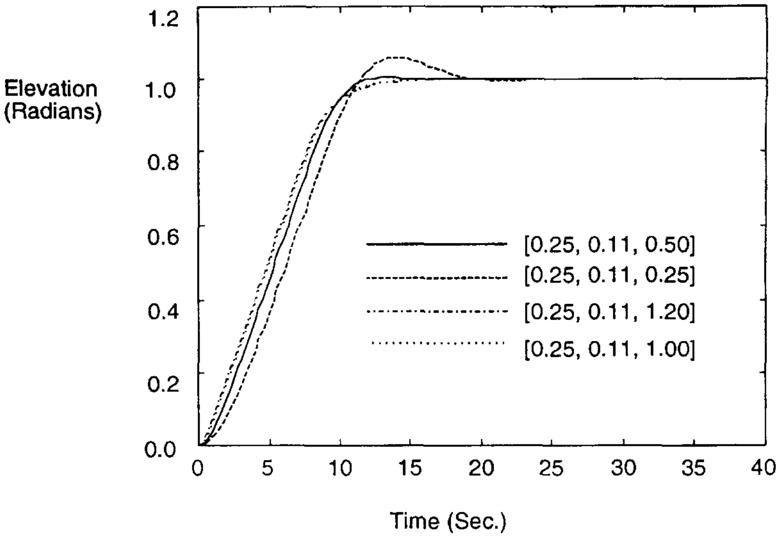

Fig. 16. Payload elevation response dùe to control support variations.

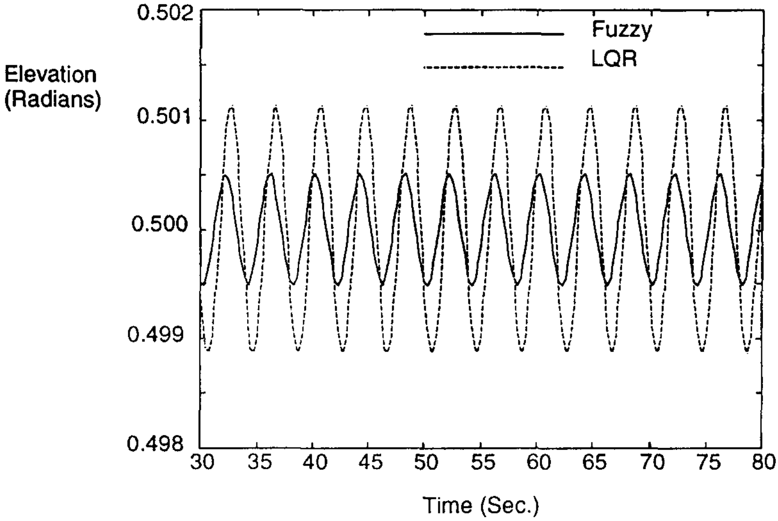

Fig. 17. Payload elevation response to a periodic disturbance (0.01 ft-lb, 0.25 Hz) and commanded gimbal angle of 0.5 radians using fuzzy control and LQR control.

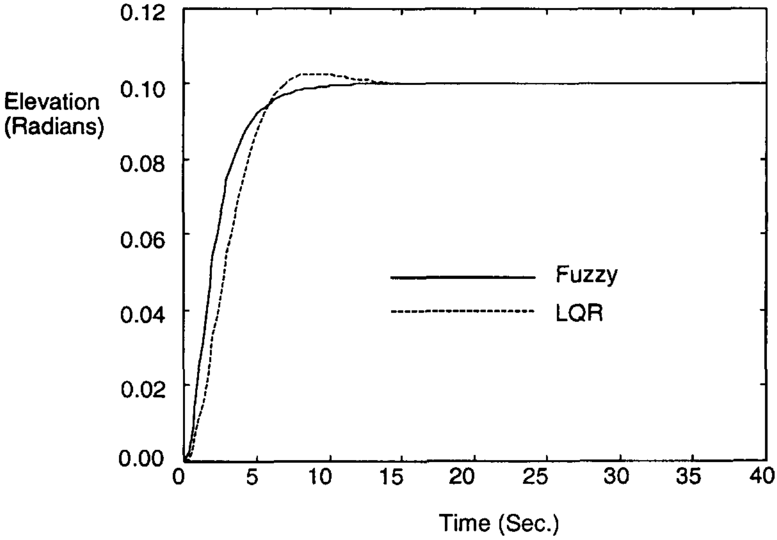

Fig. 18. Payload elevation for a commanded gimbal angle of 0.1 radians using fuzzy control and LQR control.

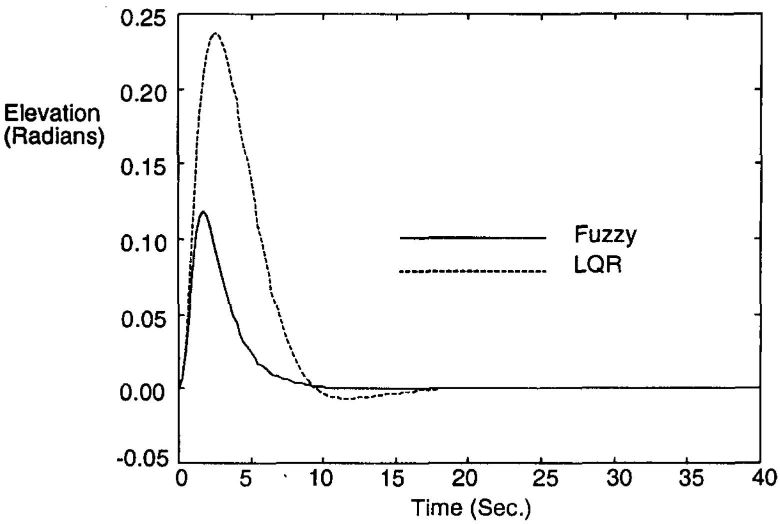

Fig. 19. Payload elevation response to a unit impulse and a commanded gimbal angle of 0.0 radians using fuzzy control and LQR control.

COMBINED DYNAMICAL RESPONSE

Once developed, the two systems and their respective controllers can be combined into a single system. The systems are dynamically coupled in two ways. The first is through the payload elevation drive shaft. Any torque which is used to drive the payload also drives the platform, but in an opposite direction. The second coupling is due to platform attitude changes. The line-of-sight pointing of the payload is the combination of the payload elevation and the platform's attitude. The coupling is illustrated in Figure 6. The results of commanding the payload to transition and maintaining 57.3 degrees are shown in Figure 22 and Figure 23. The platform response is shown for two different fuzzy controllers. The support elements for each controller are annotated in the figure. The fuzzy controller designed specifically for attitude control (with support limits [1.0E-5, 8.0E-6, 0.25]), Figure 22, does much better in correcting for the change in attitude due to the payload motion. This is due to the increased sensitivity of the error and change-in-error membership functions.

The controller with support limits [1.0E-5, 8.0E-6, 0.25] results in a maximum excursion of 0.25 arc-sec. away from the commanded position.

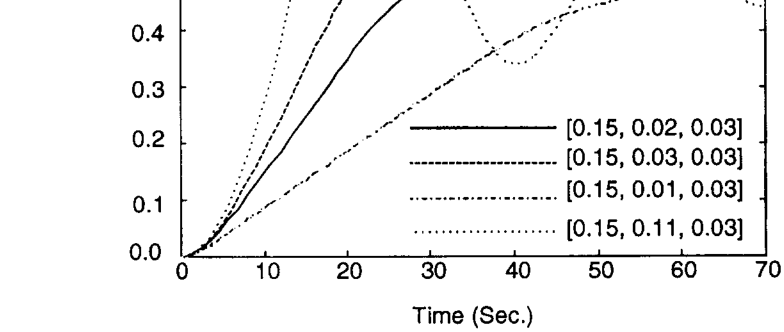

Fig. 20. Payload response to varying change-in-error support with a commanded position of 28.65 degrees (0.5 radians).

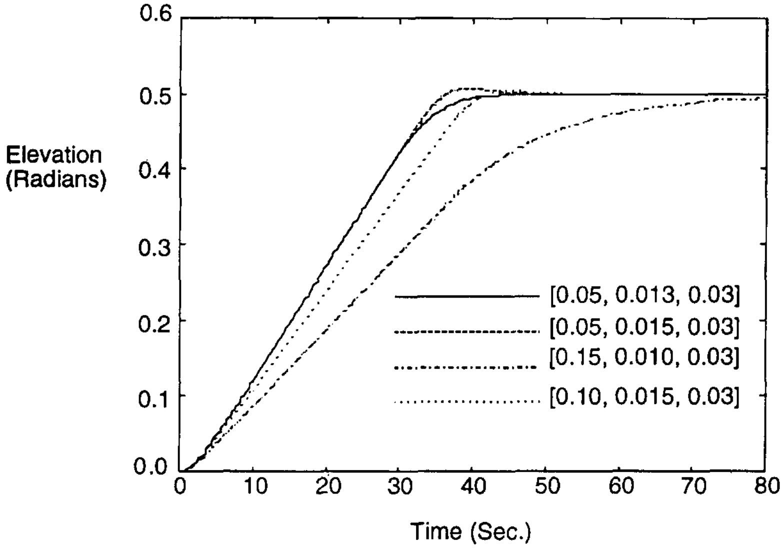

Fig. 21. Payload response to varying error support with a commanded position of 28.65 degrees (0.5 radians).

The attitude is restored to 0 arc-sec. within 10 sec. and 25 sec. for the beginning and end of the payload scew maneuver, respectively. The results of using the support limits [0.15, 0.001, 0.25] are shown in Figure 23. The attitude maximum excursion is 48 arc-sec. The controller requires over 600 sec. to maintain a commanded position of 0 arc-sec.

The curves in Figure 24 show a commanded trajectory for the payload to follow, the payload elevation, and the platform's response to the payload motion while it is following its commanded trajectory. The platform fuzzy controller is very responsive in correcting for the disturbances. A random impulse (0.03 ft-lb) is given during the payload trajectory. Both the payload and the platform were very responsive in correcting for the impulse.

The maximum platform attitude response was 0.14 arc-sec. and was due to the impulse. The maximum platform attitude response due to the payload tracking was 0.04 arc-sec. playform commanded attitude of a arc-sec. was restored within 25 sec. for all cases of disturbances.

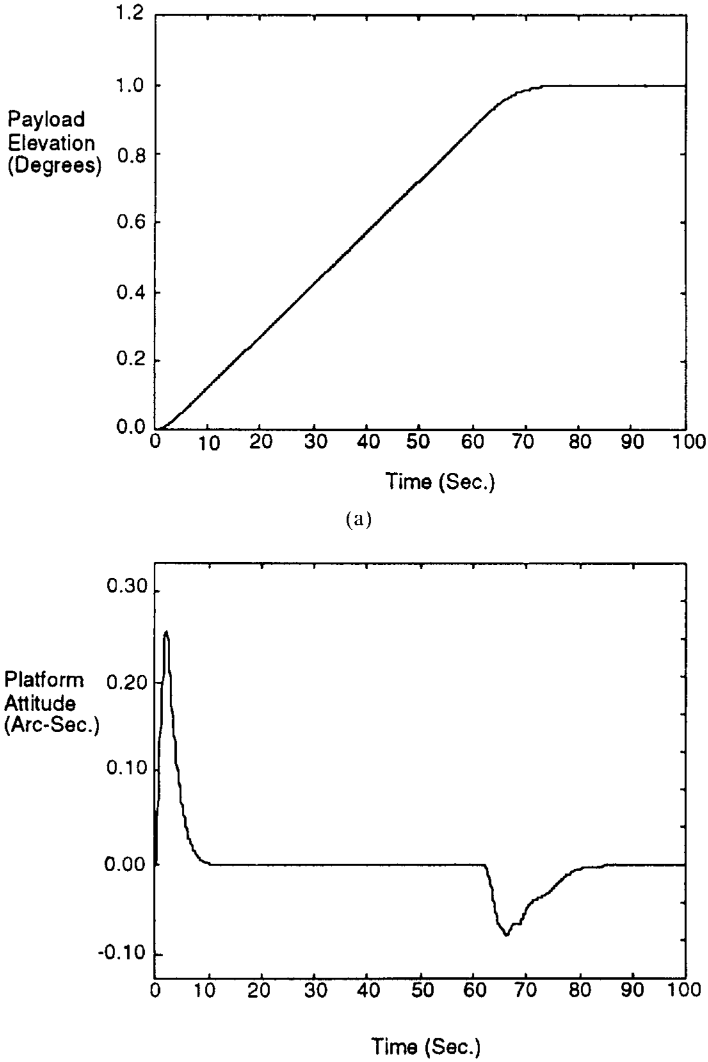

(a)

(b)

Fig. 22. a) Payload response to commanded position of 1.0 radians (57.3 deg) using support limits [0.10, 0.015, 0.03]; b) Platform response to payload commanded slew using support limits [1.0e-5, 8.0e-5, 0.25].

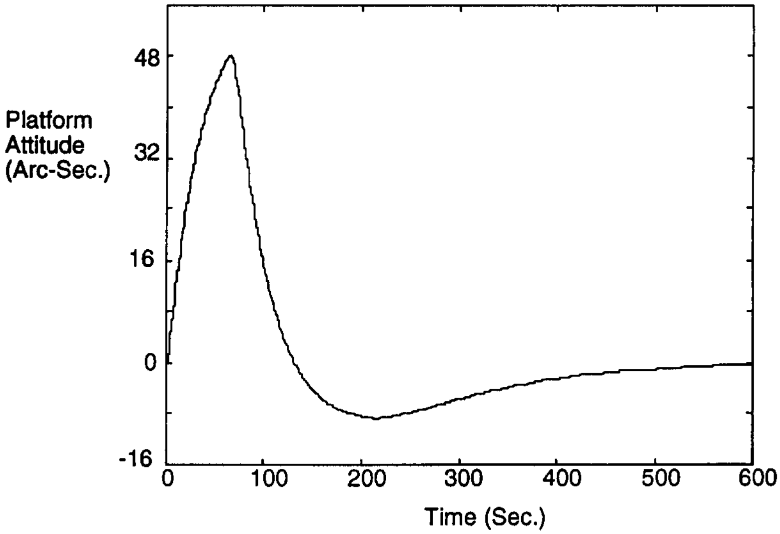

Fig. 23. Platform response to payload commanded slew using support limits [0.15, 0.001, 0.25].

CONCLUDING REMARKS

A dynamically coupled system with two autonomous fuzzy controllers has been developed. The system consisted of a space platform and a gimballed payload. The controllers are developed with the systems decoupled. Parametric studies were performed on the support limits for the error, change-in-error, and control. These parametric variations provided insight into satisfactorily tuning the controllers. The controllers were compared to controllers developed using Linear Quadratic Regulator (LQR) control design. The controllers were used to perform slew maneuvers and disturbance rejection. The fuzzy controller was more robust to variation of inertia. The robustness demonstrated that the fuzzy controller could be used when model and/or system dynamics were questionable. In all cases, the fuzzy controllers outperformed the LQR controllers.

A design procedure using constraints due to hardware or software specification was also examined. When error and control support limits are specified, tuning the fuzzy controller is made relatively easy.

The systems were coupled and the response of the payload and platform were examined for commanded payload trajectories and impulses applied to the platform. The fuzzy controllers performed very well in all cases.

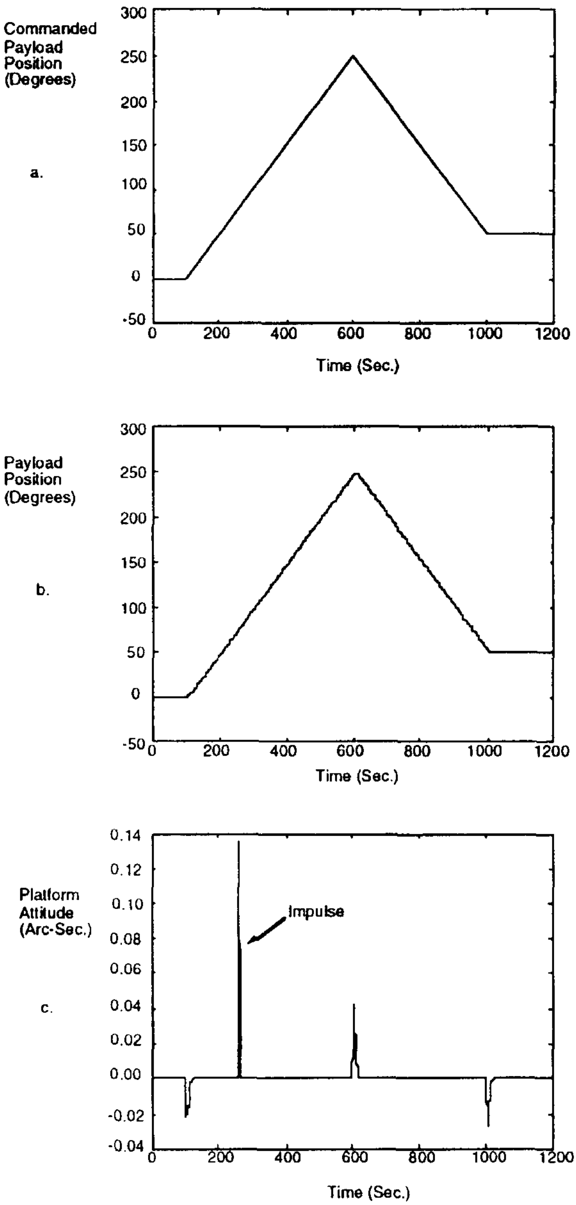

Fig. 24. a) Payload commanded slew trajectory; b) Payload response to commanded slew trajectory; c) Platform response to payload commanded slew trajectory and random impulse.

REFERENCES

1. S. E. Woodard, M. Garnek, J. D. Molnar, and W. L. Grantham, "The Upper Atmosphere Research Satellite Jitter Study," Flight Experiments Technical Interchange Meeting, Monterey, CA, Oct. 5–9, 1992.
2. A. J. Butterfield and S. E. Woodard, "Payload-payload interaction and structure-payload interaction observed on the Upper Atmosphere Research Satellite," AAS/AIAA Astrodynamics Specialist Conf., Victoria, B.C., Canada, Aug. 16–19, 1993.
3. J. Molnar and M. Garnek, "UARS in-flight jitter study for EOS," NASA Contractor Report 191419, Jan. 1993.
4. W. L. Grantham, "NASA future mission needs and benefits of controls-structures interaction technology," NASA Technical Memorandum 104034, Jan. 1991.
5. G. L. Ketner, "Survey of historical incidences with controls-structures interaction and recommended technology improvements needed to put hardware in space," Pacific Northwest Laboratory, PNL-6846, Mar. 1989.
6. L. Zadeh, "Fuzzy sets," Inform. and Control 8:338–353 (1965).
7. C. C. Lee, "Fuzzy logic in control systems: Fuzzy logic controller—Part 1," *IEEE Trans. Systems, Man, and Cybernetics* 20(2):404–418 (Mar./Apr. 1990).
8. C. C. Lee, "Fuzzy logic in control systems: Fuzzy logic controller—Part 2," *IEEE Trans. Systems, Man, and Cybernetics* 20(2):419–435 (Mar./Apr. 1990).
9. L. Zadeh, "Fuzzy logic," *IEEE Computer* 21:83–93 (Apr. 1988).
10. G. B. Cunningham, E. A. Horstkotte, and D. C. Bochsler, "Integrating fuzzy logic technology into control systems," in *Proc. AIAA Guidance, Navigation and Control Conf.*, New Orleans, LA, Aug. 12–14, 1991, pp. 1699–1702.
11. D. G. Schwartz, "Japanese advances in fuzzy systems and case-based reasoning," National Technical Information Service, No. PB92-115443, Nov. 1991.
12. R. N. Lea and Y. Jani, "Fuzzy logic in autonomous orbital operations," in *Proc. 2nd Joint Technology Workshop on Neural Networks and Fuzzy Logic*, Vol. 2, NASA Conference Publication 10061, Feb. 1991, pp. 81–110.
13. R. N. Lea, J. Hoblit, and Y. Jani, "A fuzzy logic based spacecraft controller for six degree of freedom control and performance results," in *Proc. AIAA Guidance, Navigation and Control Conf.*, New Orleans, LA, Aug. 12–14, 1991, pp. 1680–1690.
14. K. Hirota, "Research activities and industrial applications of fuzzy technology in Japan," in *Advances in Fuzzy Theory and Technology*, P. P. Wang (Ed.), Bookwrights Press, Durham, NC, 1993, pp. 269–282.
15. J. Aldrige, J. Yashvant, and T. Zafar, "Tuning fuzzy controllers for electric motors," in *Proc. 3rd Int. Symp. on Measurement and Controls in Robotics*, Torino, Italy, Sept. 21–24, 1993, pp. I-49–I-53.

Received 1 May 1994; revised 10 October 1994, 19 February 1995